

RESEARCH ARTICLE

# Selective Cytotoxicity of 1,3,4-Thiadiazolium Mesoionic Derivatives on Hepatocarcinoma Cells (HepG2)

Gustavo Jabor Gozzi<sup>1</sup>\*, Amanda do Rocio Andrade Pires<sup>1</sup>\*, Glaucio Valdameri<sup>1</sup>, Maria Eliane Merlin Rocha<sup>1</sup>, Glaucia Regina Martinez<sup>1</sup>, Guilhermina Rodrigues Noletto<sup>1</sup>, Alexandra Acco<sup>2</sup>, Carlos Eduardo Alves de Souza<sup>2</sup>, Aurea Echevarria<sup>3</sup>, Camilla Moretto dos Reis<sup>3</sup>, Attilio Di Pietro<sup>4</sup>, Silvia Maria Suter Correia Cadena<sup>1</sup>\*

**1** Departamento de Bioquímica e Biologia Molecular, Universidade Federal do Paraná, Curitiba, Paraná, Brazil, **2** Departamento de Farmacologia, Universidade Federal do Paraná, Curitiba, Paraná, Brazil, **3** Departamento de Química, Universidade Federal Rural do Rio de Janeiro, Rio de Janeiro, Brazil, **4** Equipe Labellisée Ligue 2014, BMSI UMR 5086 CNRS/Université Lyon 1, IBCP, Lyon, France

\* These authors contributed equally to this work.

\* [silvia.cadena@ufpr.br](mailto:silvia.cadena@ufpr.br)



**OPEN ACCESS**

**Citation:** Gozzi GJ, Pires AdRA, Valdameri G, Rocha MEM, Martinez GR, Noletto GR, et al. (2015) Selective Cytotoxicity of 1,3,4-Thiadiazolium Mesoionic Derivatives on Hepatocarcinoma Cells (HepG2). PLoS ONE 10(6): e0130046. doi:10.1371/journal.pone.0130046

**Academic Editor:** Matias A Avila, University of Navarra School of Medicine and Center for Applied Medical Research (CIMA), SPAIN

**Received:** March 3, 2015

**Accepted:** May 15, 2015

**Published:** June 17, 2015

**Copyright:** © 2015 Gozzi et al. This is an open access article distributed under the terms of the [Creative Commons Attribution License](https://creativecommons.org/licenses/by/4.0/), which permits unrestricted use, distribution, and reproduction in any medium, provided the original author and source are credited.

**Data Availability Statement:** All relevant data are within the paper.

**Funding:** This study was supported by the Brazilian research funding agencies CNPq (Conselho Nacional para o Desenvolvimento Científico e Tecnológico), CAPES (Coordenação de Aperfeiçoamento de Pessoal de Nível Superior), and the French National League against Cancer (Equipe Labellisée 2014), CNRS and University of Lyon 1 (UMR5086). G.J.G. was supported by a sandwich Ph.D. fellowship from the Brazilian Agency (CNPq) (process numbers

## Abstract

In this work, we evaluated the cytotoxicity of mesoionic 4-phenyl-5-(2-Y, 4-X or 4-X-cinnamoyl)-1,3,4-thiadiazolium-2-phenylamine chloride derivatives (MI-J: X=OH, Y=H; MI-D: X=NO<sub>2</sub>, Y=H; MI-4F: X=F, Y=H; MI-2,4diF: X=Y=F) on human hepatocellular carcinoma (HepG2), and non-tumor cells (rat hepatocytes) for comparison. MI-J, M-4F and MI-2,4diF reduced HepG2 viability by ~ 50% at 25 µM after 24-h treatment, whereas MI-D required a 50 µM concentration, as shown by 3-(4,5-dimethylthiazol-2-yl)-2,5-diphenyltetrazolium bromide assays. The cytotoxicity was confirmed with lactate dehydrogenase assay, of which activity was increased by 55, 24 and 16% for MI-J, MI-4F and MI-2,4diF respectively (at 25 µM after 24 h). To identify the death pathway related to cytotoxicity, the HepG2 cells treated by mesoionic compounds were labeled with both annexin V and PI, and analyzed by flow cytometry. All compounds increased the number of doubly-stained cells at 25 µM after 24 h: by 76% for MI-J, 25% for MI-4F and MI-2,4diF, and 11% for MI-D. It was also verified that increased DNA fragmentation occurred upon MI-J, MI-4F and MI-2,4diF treatments (by 12%, 9% and 8%, respectively, at 25 µM after 24 h). These compounds were only weakly, or not at all, transported by the main multidrug transporters, P-glycoprotein, ABCG2 and MRP1, and were able to slightly inhibit their drug-transport activity. It may be concluded that 1,3,4-thiadiazolium compounds, especially the hydroxy derivative MI-J, constitute promising candidates for future investigations on *in-vivo* treatment of hepatocellular carcinoma.

## Introduction

Liver cancer is the third most common cause of cancer-related death worldwide [1, 2] Hepatocellular carcinoma (HCC), specifically, represents the major histological subtype among primary

245762/2012-4). G.R.M. also received financial support from the Instituto do Milênio: Redoxoma, INCT de Processos Redox em Biomedicina—Redoxoma.

**Competing Interests:** The authors have declared that no competing interests exist.

liver cancer [1, 3], being one of the most prevalent malignant tumor worldwide [1]. Surgical resection and transplantation still remain the first choice of HCC treatment with potential cure, but this procedure must be used only in patients with early stages of HCC [4, 5]. Unfortunately, diagnosis often occurs in HCC advanced stages [2], and there is then only one—drug approved by Food and Drug Administration (FDA) that can be used as a systemic therapeutic agent for HCC treatment [6]. Other drug-based therapies have promisingly emerged as alternatives for early- and advanced- HCC treatment, which has motivated the research of new compounds to be used in patients who are not candidates to surgical treatment [5–7]. The high toxicity of drugs toward non-tumoral cells and the resistance to treatment constitute great problems in present chemotherapy [8, 9]. Drug toxicity usually limits the concentration usable for the treatments, as well as the frequency of administrations, further affecting curing efficiency [10]. Additionally, tumor cells may become resistant to drugs through different mechanisms. The most notable one is the overexpression of ATP-binding cassette transporters, such as P-glycoprotein (Pgp) [11], multidrug resistance protein 1 (MRP1) [12] and breast cancer resistant protein (ABCG2) [13], which efflux several types of drugs with unrelated structures and mechanisms [14]. This feature is a main obstacle to effectiveness of chemotherapy against HCC [15]. Indeed, several studies have demonstrated a relationship between overexpression of these efflux pumps and either poor prognosis or aggressive tumor phenotype in patients with HCC [16–18]. Mesoionic compounds with a 1,3,4-thiadiazolium ring have shown important biological activities as antibiotic [19], antiparasitic [20], antiviral [21], anticonvulsant [22], antidepressant [23], antioxidant [24], analgesic, antiinflammatory [25] and antitumoral [26] agents. We have specifically studied several 1,3,4-thiadiazolium-2-phenylamine chlorides mesoionic derivatives, only differing through the substituents of the cinnamoyl ring: MI-D, X = NO<sub>2</sub>; MI-J, X = OH; MI-4F, X = F; MI-2,4diF, X = Y = F (Fig 1). Some of them have demonstrated antitumoral effects against carcinoma, sarcoma [27] and melanoma [26, 28] tumors *in vivo*, and cytotoxic activities against several types of tumor cells have been described *in vitro* [29]. Otherwise, it has been shown that these derivatives promote functional and structural alterations in isolated rat liver mitochondria, up to different degrees depending on cinnamoyl ring substitution [30–33]. We evaluated the cytotoxicity of MI-D, MI-J, MI-4F and MI-2,4diF on human hepatocellular carcinoma cells (HepG2), and primary rat hepatocytes as a non-tumoral model, and their effects on the multi-drug resistance proteins Pgp, ABCG2 and MRP1. It was found that these compounds might represent new alternatives for HCC chemotherapeutic treatments, overcoming important limiting problems such as drug resistance and toxicity toward non-tumoral cells.

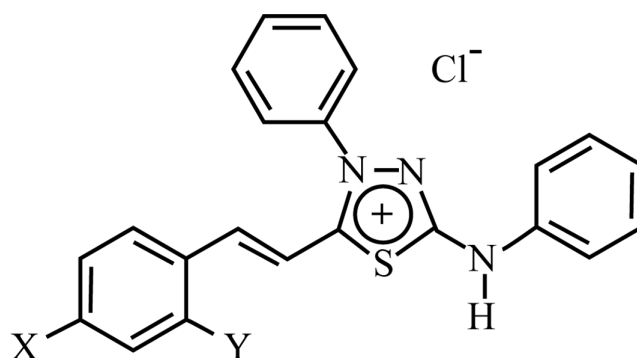


**Fig 1. Chemical structure of the 4-phenyl-5-(2-Y-4-X-cinnamoyl)-1,3,4-thiadiazolium-2-phenylamine chloride derivatives: MI-D (X = NO<sub>2</sub>; Y = H), MI-J (X = OH; Y = H), MI-4F (X = F; Y = H), and MI-2,4diF (X = Y = F).**

doi:10.1371/journal.pone.0130046.g001

## Materials and Methods

### 2.1 Chemicals

High-glucose Dulbecco's modified Eagle's medium (DMEM) was obtained from Cultilab (Campinas, Brazil) and fetal bovine serum (FBS) was purchased from Gibco. Dimethylsulfoxide (DMSO) was obtained from Merck (São Paulo, SP, Brazil). Annexin V Apoptosis Detection Kit was purchased from BD Bioscience (São Paulo, SP, Brazil). Lactate dehydrogenase (LDH) detection kit (Liquiform) was obtained from Labtest (Lagoa Santa, MG, Brazil). Bovine serum albumin (BSA), 3-(4,5-dimethylthiazol-2-yl)-2,5-diphenyltetrazolium bromide (MTT) and 4-(2-hydroxyethyl)-1-piperazine ethanesulfonic acid (HEPES) were purchased from Sigma. All other reagents were commercial products of the highest available purity grade. The mesoionic derivatives, MI-D (4-phenyl-5-(4-nitrocinnamoyl)-1,3,4-thiadiazolium-2-phenylamine chloride), MI-J (4-phenyl-5-(4-hydroxycinnamoyl)-1,3,4-thiadiazolium-2-phenylamine chloride), MI-4F (4-phenyl-5-(4-fluorocinnamoyl)-1,3,4-thiadiazolium-2-phenylamine chloride), MI-2,4diF (4-phenyl-5-(2,4-fluorocinnamoyl)-1,3,4-thiadiazolium-2-phenylamine chloride), were synthesized by the Department of Chemistry of the Federal Rural University of Rio de Janeiro, Brazil, and their structures were confirmed by  $^1\text{H}$  NMR,  $^{13}\text{C}$  NMR and mass spectrometry [34]. For this study, the derivatives were dissolved in DMSO and then further diluted with the assay medium. Controls with DMSO (maximal 0.7%, v/v) were carried out in each assay.

### 2.2 HepG2 cell culture

The human hepatocarcinoma HepG2 cell line (from the American Type Culture Collection—ATCC) was maintained in high-glucose DMEM supplemented with 10% FBS, 100 UI/mL penicillin G and 100  $\mu\text{g}/\text{mL}$  streptomycin, 20 mmol/L 4-(2-hydroxyethyl)-1-piperazine ethanesulfonic acid (HEPES), adjusted to pH 7.4 with 1 mol/L sodium bicarbonate. HepG2 cells were grown in poly-L-lysine-coated flasks at 37°C, 5%  $\text{CO}_2$  under controlled humidity. Sub-culturing was performed at approximately 48 h intervals, and cell growth was monitored with an Olympus inverted microscope.

### 2.3 Primary culture of rat hepatocytes

**2.3.1 Animals.** Male Wistar rats (180–200 g) were obtained from the Central Animal House of the Federal University of Paraná (PR, Brazil). The animals received a standard laboratory diet (Purina) and tap water. This study was carried out in strict accordance with the recommendations in the Guide for the Care and Use of Laboratory Animals of the National Institutes of Health. The protocol was approved by the Committee on the Ethics of Animal Experiments of the University Federal of Paraná (Permit Number: 548). All surgery was performed under ketamine/xylazine anesthesia, and all efforts were made to minimize suffering.

**2.3.2 Isolation and culture of hepatocytes.** The hepatocytes were obtained by monovascular liver perfusion of Wistar rats, as described previously by [35, 36] with some modifications. The male rats were weighed and anesthetized intraperitoneally with a mixture of ketamine (60 mg/kg) and xylazine (7.5 mg/kg). Following laparotomy, 100  $\mu\text{L}$  of sodium heparin (5000 U/mL) were injected into the abdominal cava vein. The portal and thoracic cava veins were cannulated, and the liver was perfused for 10–15 min with Krebs solution (2.4 mol/L NaCl, 96 mmol/L KCl, 24 mmol/L  $\text{KH}_2\text{PO}_4$ , 24 mmol/L  $\text{MgSO}_4$ , 480 mmol/L  $\text{NaHCO}_3$  and 1 mol/L HEPES buffer, pH 7.4) containing 1.3 mol/L  $\text{CaCl}_2$ , 20 mg collagenase (types IA and IV) and carbogen (95%  $\text{O}_2$ :5%  $\text{CO}_2$ ). The liver was excised, and the cells were released by mechanical action, filtered through 50- $\mu\text{m}$  nylon membranes and centrifuged at 400 rpm for 5 min at 4°C. Subsequently, the cells were centrifuged four times with Krebs solution

supplemented with 20% BSA and treated with carbogen. The cells were suspended in high-glucose DMEM supplemented with FBS (10%), insulin (100 nmol/L), glucagon (10 nmol/L), epidermal growth factor (10 ng/mL), dexamethasone (50 nmol/L), penicillin (100 U/mL) and streptomycin (100 ng/mL). Cell viability was determined using the Trypan blue (0.4%, w/v) exclusion method as previously described by Philips [37]. Only the cell suspensions with viabilities higher than 80% were plated ( $1 \times 10^6$  cells/plate on a 60 mm plate) and cultured for further experiments. For 4h after plating, the medium was replaced by Hepatozyme with or without mesoionic compounds. Considering some delays during the isolation procedure and the time required for further assays (e.g. viability assays), the time of treatment was from 18 to 24h. It is important to remark that no differences in the results were observed during this interval.

## 2.4 Culture of multiple drugs resistant cells

The human embryonic kidney (HEK293) cells stably transfected with *ABCG2* (HEK293*ABCG2*) [38] or *MRP1* (HEK293*ABCC1*), and their respective parental HEK293 (wild-type) or HEK293*pcDNA5* (empty-vector) cells, were maintained at 37°C (5% CO<sub>2</sub>) in high-glucose DMEM medium, supplemented with 10% fetal bovine serum, 1% penicillin/streptomycin. The mouse embryonic fibroblasts, of either wild-type (NIH3T3) or overexpressing Pgp (NIH3T3*ABCB1*) [39], were maintained under the same conditions. The cell culture media were drug supplemented with either 0.75 mg/mL G418 (HEK293*ABCG2*), 200 µg/mL hygromycin B (HEK293*pcDNA5* and HEK293*ABCC1*) or 60 ng/mL colchicin (NIH3T3*ABCB1*).

## 2.5 Cell viability assays

**2.5.1 MTT reduction.** HepG2 cells were seeded at a density of  $1 \times 10^4$  cells/well into 96-well culture plates. After 24 h, the cells were treated with mesoionic compounds at concentrations of 5, 25 and 50 µM for 24 h. Hepatocytes were seeded at  $1 \times 10^6$  cells/plate in 60-mm plates, and treated with compounds at 25 µM up to 18–24 h. Cell viability was evaluated through the MTT assay [40, 41], and the absorbance was determined at 550 nm. The results were expressed as a percentage of viable cells in comparison to the control (taken as 100%). All HEK293 cells were seeded at a density of  $1 \times 10^4$  cells/well into 96-well culture plates, and incubated for 24 h at 37°C in 5% CO<sub>2</sub>. NIH–3T3 and NIH–3T3*ABCB1* cells were seeded at a density of  $3.5 \times 10^3$  and  $5.0 \times 10^3$  cells/well, respectively, and maintained under the same conditions before treatment. The cells were treated with mesoionic derivatives for 72 h; then, 20 µL of MTT solution (5 mg/mL) were added to each well and incubated for 4 h at 37°C. The culture medium was discarded, and 100 µL of a DMSO:ethanol (1:1) solution was added into each well and mixed by gently shaking for 10 min. Absorbance was measured in a microplate reader at 570 nm, from which the value measured at 690 nm was subtracted.

**2.5.2 Lactate dehydrogenase release.** HepG2 and hepatocytes cells were plated and treated as described in the item 2.4.1. Aliquots (50 µL) of culture medium were centrifuged at 1000 rpm for 5 min, and LDH activity was measured by monitoring the decrease of NADH at 340 nm, with the LDH kit assay, according to manufacturer instructions.

**2.5.3 Annexin-V and propidium iodide staining.** HepG2 cells were seeded at a density of  $1 \times 10^6$  cells in 60-mm plates, and treated with mesoionic derivatives at 25 µM for 24 h. At the end of exposure, cells were collected by trypsinization, centrifuged at 300xg for 5 min at 4°C and suspended in 500 µL of binding buffer (10 mM Hepes, pH 7.4, 150 mM NaCl, 5mM KCl, 1 mM MgCl<sub>2</sub> and 1.8 mM CaCl<sub>2</sub>). Aliquots (100 µl) of the cell suspension were incubated with 5 µl of the reagent mixture containing annexin V-FITC conjugate (BD Pharmingen) and 10 µl of propidium iodide (PI) (50 µg/mL) for 15 min at 25°C. After incubation, 400 µl of binding



buffer were added and the cells were analyzed by flow cytometry [42]. Positive controls were separately stained with Annexin V alone (channel FL-1), PI alone (channel FL-2), and both markers, for compensation settings of the two signals. Flow cytometric analysis was carried out on a FACSCalibur flow cytometer (BD Biosciences Pharmingen, San Diego, CA, USA). In each sample, 10,000 events were recorded and analysis was performed using the WinMDI 2.9 software. Three independent experiments were performed for each treatment condition. Hepatocytes were seeded at  $1 \times 10^6$  cells/plate in 60-mm plates, and treated with compounds at 25  $\mu$ M up to 18–24 h. The culture medium was then replaced by the binding buffer containing 5  $\mu$ l of annexin-V FITC and 0.8 mg/mL of PI. Cells were analyzed by fluorescence microscopy (AXIOVERT 40CSFL) with a 10X objective, in either absence (visible) or presence of annexin filter—FL1: 515–530 nm or PI-FL2: 560–580 nm.

## 2.6 Morphology assays

HepG2 cells ( $1 \times 10^5$  cells/well) were seeded in 24-well plates with glass slides on the bottom, and incubated in a humidified incubator with 5% CO<sub>2</sub> and at 37°C for 24 h. After adhesion, the medium was replaced by new medium with or without mesoionic derivatives at 5  $\mu$ M for 3 h. The cells were fixed with Bouin solution (formaldehyde at 4% (v/v):saturated picric acid:glacial acetic acid, 4:15:1) for 5 min at ambient temperature. Then, the cells were washed with ultra-pure water, and stained with hematoxylin and eosin. They were dehydrated with acetone and xylol solutions, and assembled with Entelan (Merck). The morphological alterations were viewed in Bel Fotonics microscope with 40 X and 100 X magnification, and the images were captured by a photographic camera Sony Cyber-Shot at 13.5 mega pixels. Hepatocytes were seeded at  $1 \times 10^6$  cells/plate in 60-mm and treated with compounds at 25  $\mu$ M up to 18–24 h. After exposure, the morphology was analyzed by optical microscopy (AXIOVERT 40CSFL) with a 20X objective.

## 2.7 DNA fragmentation

The fragmented DNA content was determined by flow cytometry using PI [43–45]. For these assays,  $1 \times 10^6$  cells were dispensed in 60-mm plates, and incubated for 24 h for adhesion at 37°C in 5% CO<sub>2</sub>. The culture medium was then replaced by fresh medium without (control) or with 25  $\mu$ M derivatives, or the corresponding volumes of DMSO, and further incubated for 6 and 24 h. After incubation, the culture medium and cells were collected in a Falcon tube by trypsinization, and the samples were centrifuged at 2000 rpm for 5 min. The precipitate was suspended in phosphate buffered saline (PBS) and centrifuged again under the same conditions. The cells were suspended in 0.3 mL of a solution composed of 50  $\mu$ g/mL of propidium iodide and 0.1% Triton X -100 in PBS. After labeling, the cells were kept in the dark and analyzed by flow cytometry with the FACSCalibur (BD) apparatus using Cell Quest program. The data acquisition was done using the FL2 filter (yellow fluorescence), and analyzed as histograms (FL2 *versus* number of events). The number of cells in each phase of the cell cycle was expressed as a percentage of total events (10,000 cells). Histograms were analyzed using the WinMDI 2.9 software.

## 2.8 Protein concentration assay

Protein concentration was determined by the method of Bradford [46] using bovine serum albumin BSA as a standard.

## 2.9 Inhibition of drug efflux in multiple drug resistant cells

HEK293ABC $G_2$  cells were seeded at a density of  $1.0 \times 10^5$  cells/well into 24-well culture plates. After 72-h incubation, they were exposed to 5  $\mu\text{M}$  mitoxantrone for 30 min at 37°C, in the presence or absence of each derivative, and then washed with PBS and trypsinized. The intracellular fluorescence was monitored with a FACSCalibur cytometer (Becton Dickinson), using the FL4 channel and at least 10,000 events were collected. The percentage of inhibition was calculated relatively to 1  $\mu\text{M}$  Ko143 which produced a complete inhibition. NIH-3T3ABC $B_1$  were seeded at a density of  $6 \times 10^4$  cells/well into 24-well culture plates and incubated for 48 h at 37°C, whereas HEK293 cells transfected with ABC $C_1$  were seeded at  $2.5 \times 10^5$  cells/well for 72 h. The cells were respectively exposed to rhodamine 123 (0.5  $\mu\text{M}$ ) or calcein-AM (0.2  $\mu\text{M}$ ) for 30 min at 37°C, in the presence or absence of each derivative, then washed with PBS and trypsinized. The intracellular fluorescence was monitored using the FL1 channel. The inhibition was measured relatively to 5  $\mu\text{M}$  GF120918 or 35  $\mu\text{M}$  verapamil, respectively, producing complete inhibitions. The percentage of inhibition was calculated by using the following equation:

$$\% \text{ inhibition} = (C - M) / (C_{ev} - M) \times 100,$$

where C corresponds to the intracellular fluorescence of resistant cells in the presence of compounds and fluorescent substrate, M to the intracellular fluorescence of resistant cells with the fluorescent substrate alone, and  $C_{ev}$  corresponds to the intracellular fluorescence of cells inhibited with standard inhibitor in the presence of fluorescent substrate.

## 2.10 Statistical Analysis

Results were expressed as mean  $\pm$  standard deviation, and subjected to analysis of variance (ANOVA) and Tukey test for comparison of means. A *P*-value lower than 0.05 was considered significant. All analyses and graphs were performed using GraphPad Prism Software version 6.0.

## Results

### 3.1 Cytotoxicity of 1,3,4-thiadiazolium derivatives on HepG2 and rat hepatocytes

The viability of HepG2 cells was determined after 24 h of treatment with derivatives at 5, 25 and 50  $\mu\text{M}$ , by both MTT and LDH-release assays. As observed in Fig 2, upper panel, MI-J, MI-4F and MI-2,4diF reduced HepG2 cells viability by about 50% at 25  $\mu\text{M}$  when analyzed by MTT. MI-D only reduced by 28% the cell viability, requiring 50  $\mu\text{M}$  to reach 50%. The results of the LDH-release assay (Fig 2, lower panel) also demonstrated the reduction of cell viability by MI-J, MI-4F and MI-2,4diF treatments. The enzymatic activity of the culture medium was increased by 55, 24 and 16%, respectively, for MI-J, MI-4F and MI-2,4diF at 25  $\mu\text{M}$ , in comparison to controls without mesoionic derivative. MI-D, on the contrary, did not significantly affect the LDH activity. The viability of primary hepatocytes was also determined in order to verify the selectivity of derivatives for tumor cells. As observed in Fig 3, no cytotoxicity was observed in MTT assays (upper panel), except for MI-2,4diF producing a 36% effect (at 25  $\mu\text{M}$  for 18–24 h). However, no increase in LDH activity was observed with any derivative (lower panel). Interestingly, MI-D induced a reduction of LDH activity (~ 17% at 25  $\mu\text{M}$ ).

### 3.2 Apoptosis induction by 1,3,4-thiadiazolium derivatives in HepG2 cancer cells but not in control hepatocytes

Considering the significant toxicity of the derivatives on HepG2 cells (Fig 2), we evaluated the induction of apoptosis in these cells by DNA fragmentation, a key event of cells undergoing

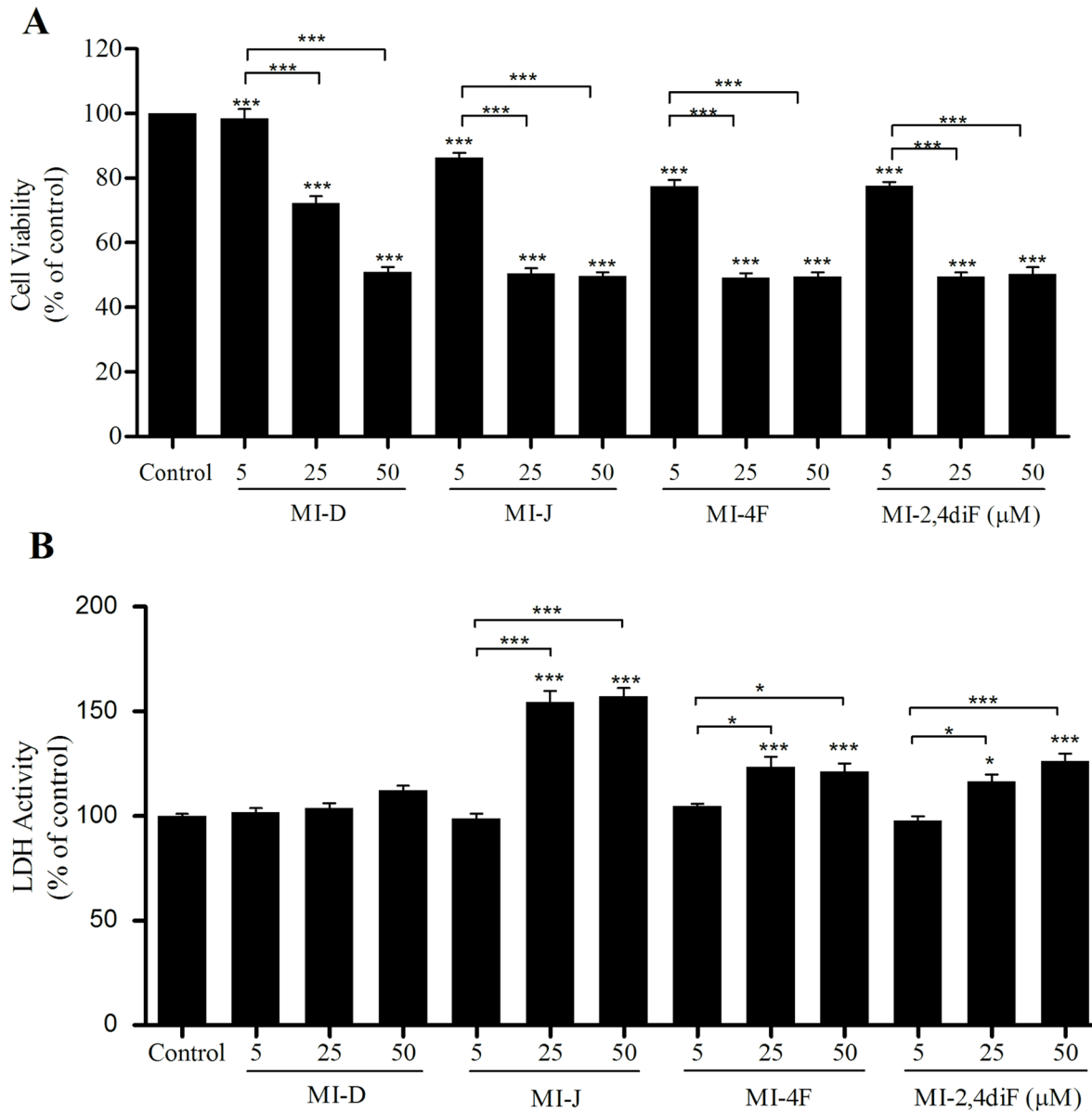


**Fig 2. Cytotoxic effects of 1,3,4-thiadiazolium derivatives on HepG2 cells.** A. MTT assay (the experimental conditions are described in the Materials and Methods section 2.5.1). The cells were seeded with or without 1,3,4-thiadiazolium derivatives at 5, 25 or 50 μM for 24 h. The results were expressed as % of viability in comparison to control. B. LDH release assay (the experimental conditions are described in the Materials and Methods section 2.5.2). Under the same treatment conditions, as described above, LDH activity was measured in supernatants. Data represent means of four different experiments in quadruplicate. The results were expressed as % of viability in comparison to control. \* and \*\*\* denote values significantly different from the control or between the different treatments at  $P < 0.05$  and  $P < 0.0001$ , respectively.

doi:10.1371/journal.pone.0130046.g002

apoptosis [47]. After 24 h of treatment with MI-J, MI-4F and MI-2,4diF (Fig 4C–4E), approximate increases of 12%, 9% and 8%, respectively, were observed, as evidenced by the higher number of cells in sub-G1 region. MI-D under the same conditions did not promote any significant alteration in DNA fragmentation, but increased the number of cells in G2/M phase (Fig 4B). The G1/G0 and G2/M phases were not significantly changed by the other derivatives. To further investigate the induction of apoptosis by mesoionic derivatives, HepG2 cells were simultaneously stained with FITC-conjugated annexin V and PI, and analyzed by flow

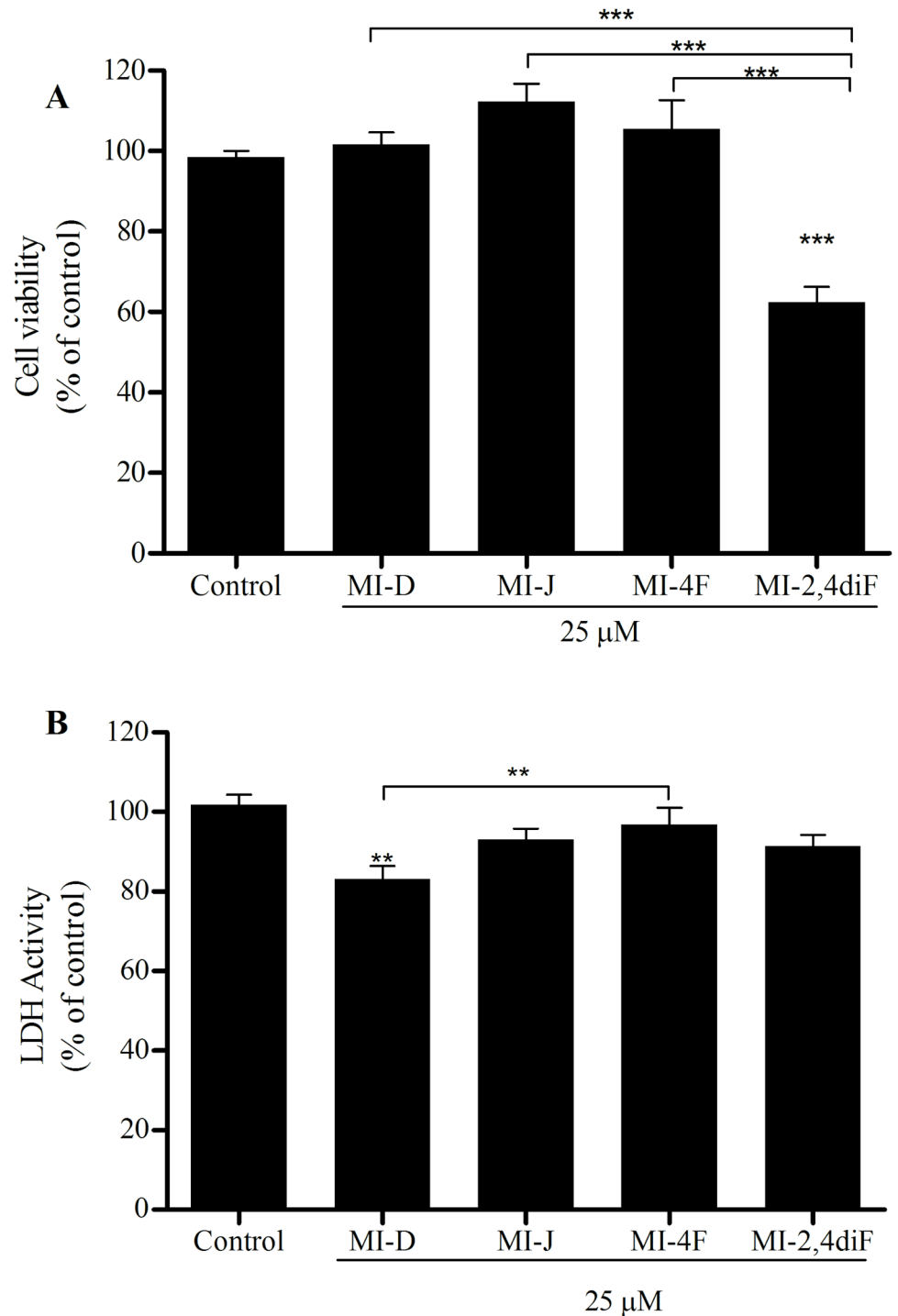


**Fig 3. Cytotoxic effects of 1,3,4-thiadiazolium derivatives on hepatocytes.** A. MTT assay (the experimental conditions are described in the Materials and Methods section 2.5.1) The cells were seeded with or without 1,3,4-thiadiazolium derivatives at 25 for 18–24 h. The results were expressed as % of viability in comparison to control. B. LDH release assay (the experimental conditions are described in the Materials and Methods section 2.5.2). Under the same treatment conditions described above, LDH activity was measured in the supernatants. Data represent means of four different experiments in quadruplicate. The results were expressed as % of viability in comparison to control. \*\* and \*\*\* denotes values significantly different from the control or between the different treatments at  $P < 0.01$  and  $P < 0.0001$ , respectively.

doi:10.1371/journal.pone.0130046.g003

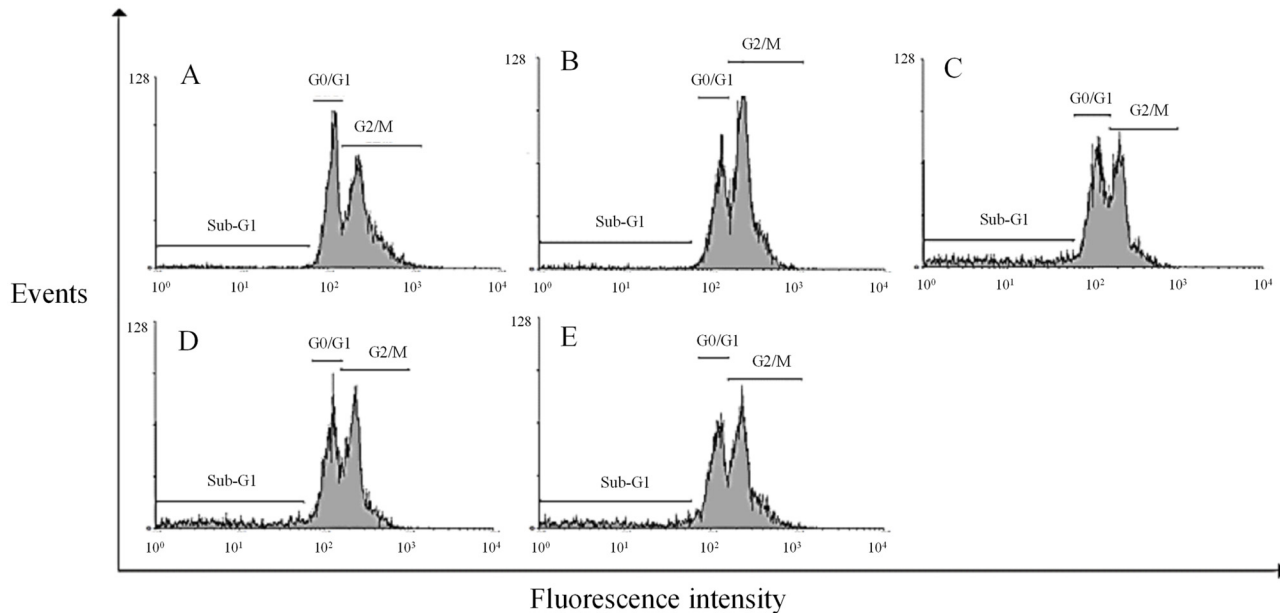


**Fig 4. DNA fragmentation in HepG2 cells, as induced by 1,3,4-thiadiazolium derivatives (the experimental conditions are described in the Materials and Methods section 2.7).** The cells were seeded with or without 1,3,4-thiadiazolium derivatives at 25  $\mu$ M for 24 h. For each sample, 10,000 events were analyzed by flow cytometry using FL2 filter. (A) control, (B) MI-D, (C) MI-J, (D) MI-4F and (E) MI-2,4diF. The histograms represent three different experiments in triplicate.

doi:10.1371/journal.pone.0130046.g004

cytometry (Fig 5). All compounds (at 25  $\mu$ M for 24 h) increased the number of doubly-stained cells in comparison to control, reaching up to 76% for MI-J, 36% and 25% for MI-4F and MI-2,4diF, while a lower value of 11% was observed for MI-D. In addition, MI-J and MI-2,4diF promoted a slight increase (around 2.4%) in the number of PI-labeled cells. Since the differentiation between apoptosis and necrosis was not possible with such an assay, short incubation time (3 h) and reduced concentration (5  $\mu$ M) were used for morphological analyzes [47]. Apoptotic bodies (blebs) were observed, and loss of cellular organization in monolayer was elicited for all compounds even at low concentration (Fig 6). Other characteristics of apoptosis induction, such as vacuolization, cellular shrinkage (with MI-D, MI-J and MI-4F) and nuclear pyknosis (with MI-4F and MI-2,4diF), were also observed. All together, these results suggest that apoptosis may be the death pathway induced by 1,3,4-thiadiazolium derivatives on HepG2 cells. Cultured hepatocytes were also doubly stained with FITC-conjugated annexin V and PI, and analyzed by fluorescence microscopy (Fig 7), but no increase in annexin-FITC and PI labeling was observed for any compound (at 25  $\mu$ M for 18–24 h) when compared to treatment with acetylsalicylic acid (at 20 mM for 18–24 h), used as a positive control [48]. The hepatocytes morphology was also verified: no alterations in normal characteristics of primary hepatocytes, as cubic form, monolayer organization and multinucleation was observed, supporting previous results suggesting that these derivatives slightly or not at all affected hepatocytes viability (Fig 8).

### 3.3 Effects of 1,3,4-thiadiazolium derivatives on multiple drugs resistant (MDR) cells

The effects of 1,3,4-thiadiazolium derivatives were checked on cells overexpressing multidrug ABC transporters, in order to establish their capacity to inhibit the transport of substrate drugs and/or to be transported themselves. Flow cytometry was used to analyze their capacity to



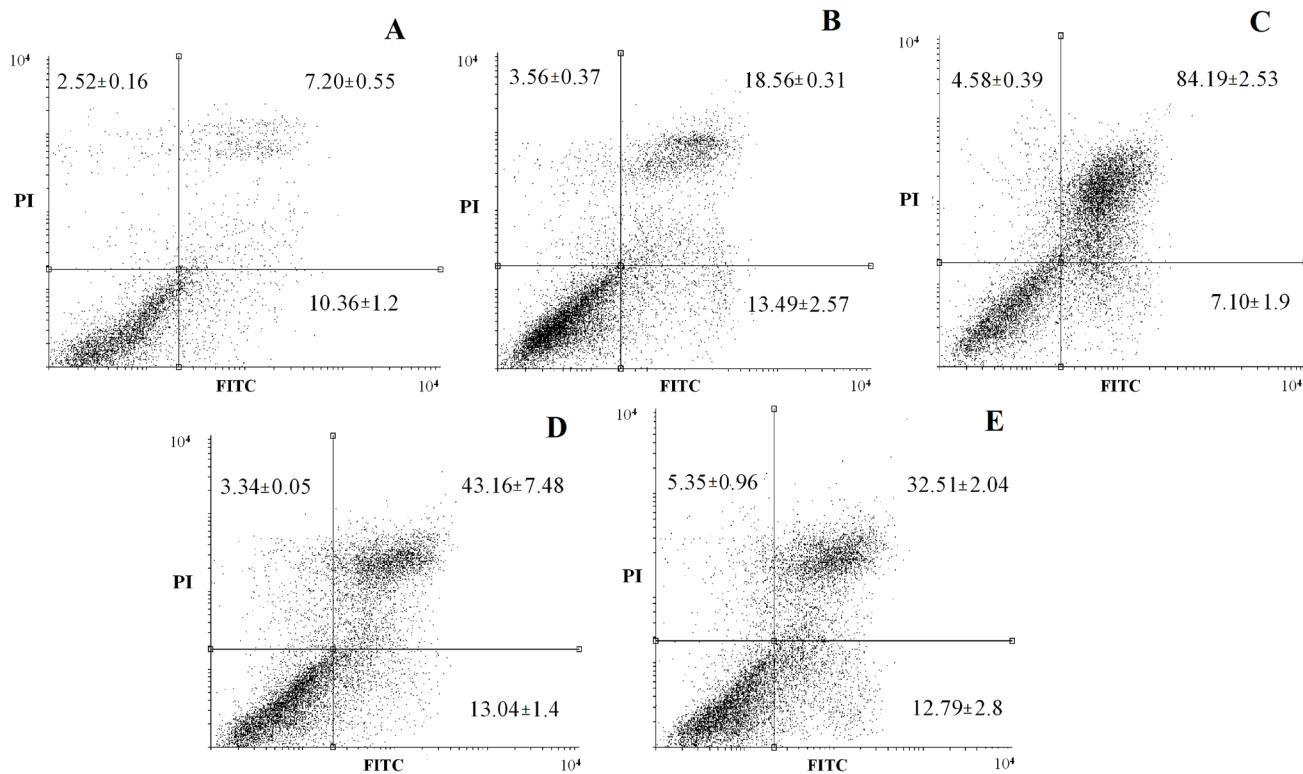


**Fig 5. Annexin V-FITC and propidium iodide staining of HepG2 treated with 1,3,4-thiadiazolium derivatives (the experimental conditions are described in the Materials and Methods section 2.5.3).** The cells were seeded with or without 1,3,4-thiadiazolium derivatives at 25  $\mu$ M for 18–24 h. Then, the cells were collected with trypsin and 10,000 events were analyzed by flow cytometry by FL2 and FL1 filters. (A) control, (B) MI-D, (C) MI-J, (D) MI-4F and (E) MI-2,4diF. The figures show representative dot-plot with the different cell populations: left-bottom = labeled cells; left-top = PI labeled; right-top = doubly labeled; right-bottom = annexin V labeled. The results were expressed as mean  $\pm$  SD of three independent experiments.

doi:10.1371/journal.pone.0130046.g005

induce accumulation of fluorescent substrates. [Table 1](#) shows that, among the different mesoionic derivatives, only MI-J was able to significantly inhibit the Pgp-mediated efflux of rhodamine 123, with 13% inhibition (at 25  $\mu$ M upon 30-min incubation) as compared to the control which was fully inhibited by 5  $\mu$ M elacridar. The ability of the derivatives to be transported by Pgp was evaluated by the resistance ratio (RR), which was obtained by dividing the  $IG_{50}$  values estimated from survival MTT assays for transfected cells overexpressing the multidrug transporter and its parental, sensitive line, with RR values  $> 1$  suggesting transporter-mediated efflux [49]. Except for MI-J which was not to be transported by Pgp, with a RR value even  $< 1$ , the other derivatives indeed appeared to be transported, with high RR values of 5.2 for MI-2,4diF, and in the range 2.4–2.8 for MI-D and MI-4F.

The same parameters were evaluated for the two other multidrug transporters, ABCG2 and MRP1. All derivatives significantly inhibited the ABCG2-mediated efflux of mitoxantrone: the extent observed at 25  $\mu$ M after 30-min incubation was higher with MI-D containing a  $NO_2$  (~37%), but the affinity appeared better for MI-J containing a OH ( $EC_{50}$  value of 8.5  $\mu$ M versus 24.3  $\mu$ M). The two fluorinated derivatives (MI-4F and MI-2,4diF) displayed a lower inhibition (11.7–17.7%). No apparent transport by ABCG2 was observed, except for a weak possible effect of MI-J, with a RR value slightly  $> 1$ . No cross resistance at all was observed with MRP1-overexpressing cells, with RR values very close to unity. The different derivatives also inhibited MRP1-mediated drug efflux, using calcein-AM as a substrate, but with different structure-activity relationships when compared to ABCG2 since OH substitution in MI-J was much

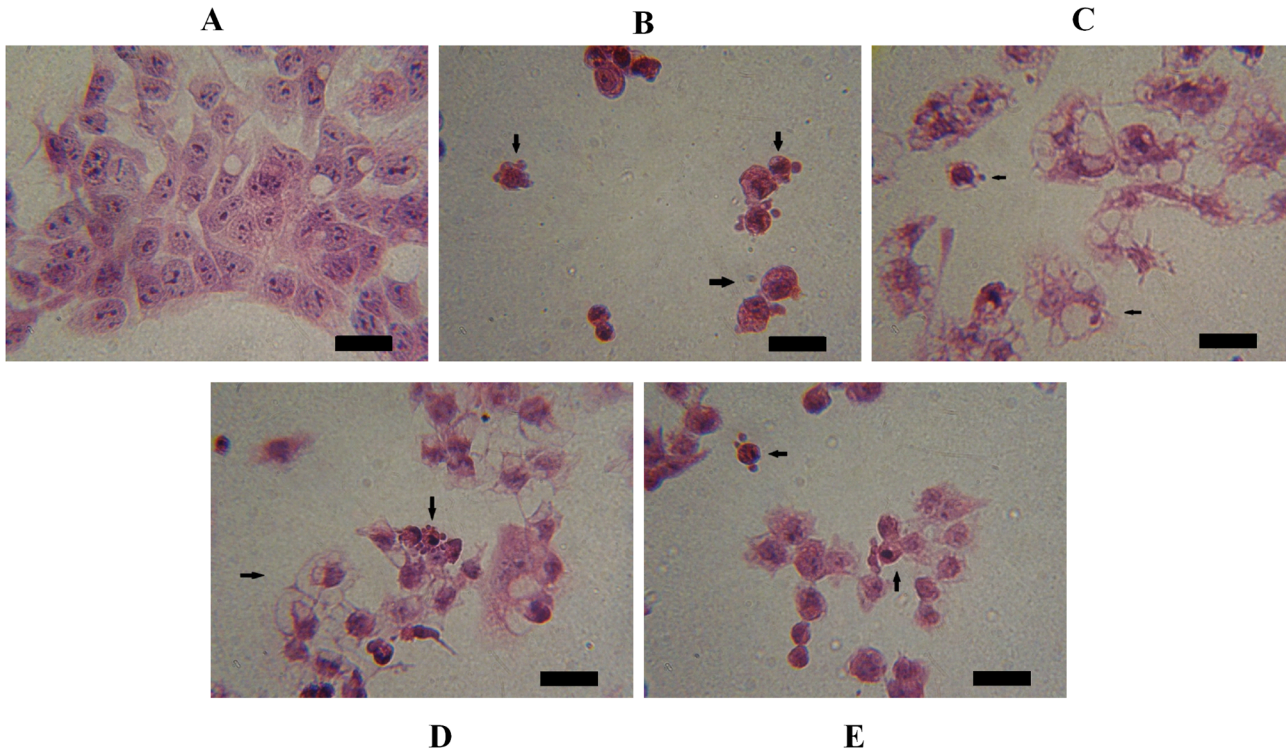


**Fig 6. Effects of 1,3,4-thiadiazolium derivatives on HepG2 cell morphology (the experimental conditions are described in the Materials and Methods section 2.6).** The cells were seeded with or without 1,3,4-thiadiazolium derivatives at 5  $\mu$ M for 3 h. The images were captured with a 100X magnification; they correspond to control (A), MI-D (B), MI-J (C), MI-4F (D) and MI-2,4diF (E). The scale is indicated by black bars representing 0.02 mm. The arrows show morphological modifications as blebs, increased volume and vacuolization. The photographs represent three different experiments in triplicate.

doi:10.1371/journal.pone.0130046.g006

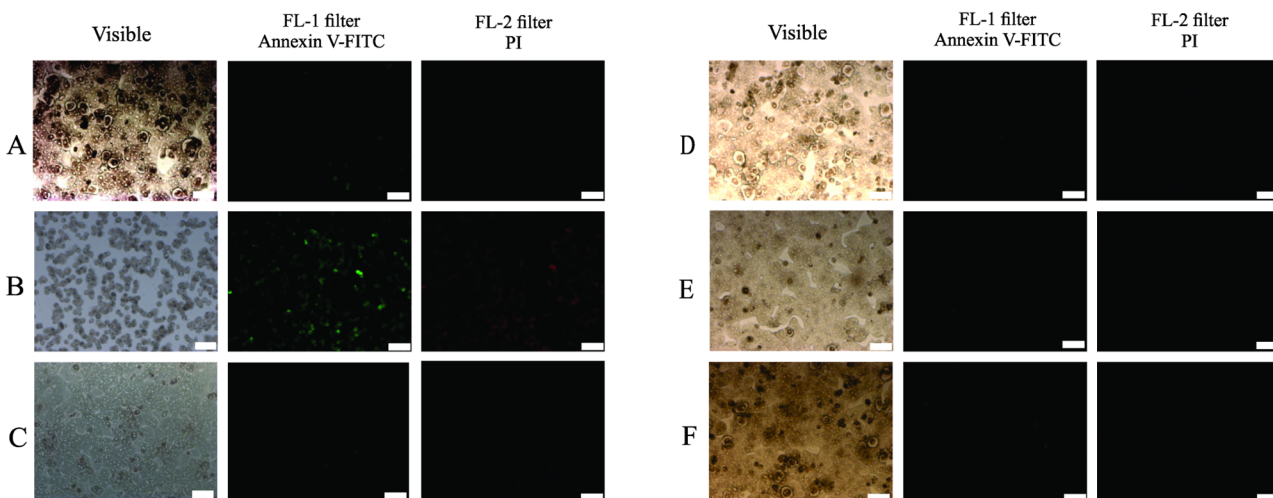


**Fig 7. Annexin V-FITC and propidium iodide staining of hepatocytes treated by 1,3,4-thiadiazolium derivatives (the experimental conditions are described in the Materials and Methods section 2.5.3).** Hepatocytes were incubated with derivatives at 25  $\mu$ M for 20 h. The images (10X magnification) were captured with an AXIOVERT 40CSFL fluorescence microscope. The scale is indicated by white bars representing 100  $\mu$ m. The annexin V-FITC-positive cells are stained in green, and the PI-positive cells in red. The images represent (A) control (untreated cells), (B) ASA positive control at 20 mM, (C) MI-D, (D) MI-J, (E) MI-4F and (F) MI-2,4diF. The figures represent three different experiments in triplicate.

doi:10.1371/journal.pone.0130046.g007



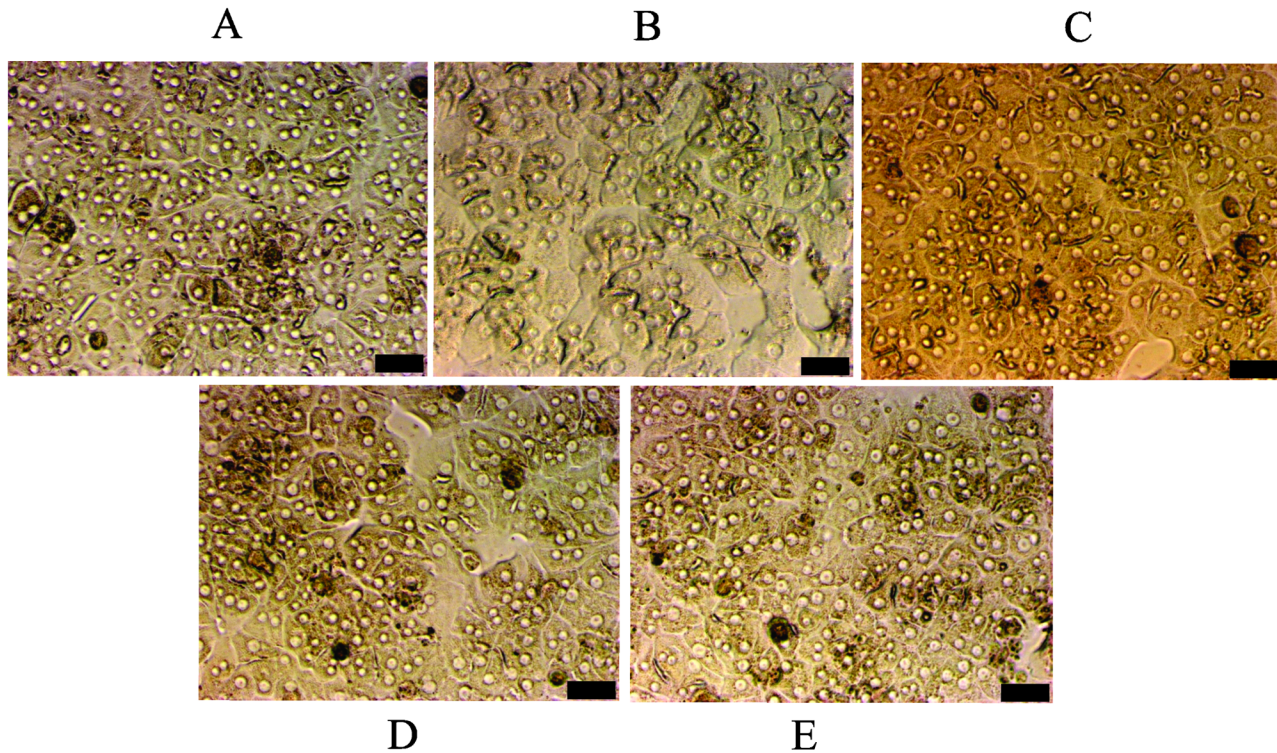


**Fig 8. Effects of 1,3,4-thiadiazolium derivatives on hepatocytes morphology (the experimental conditions are described in the Materials and Methods section 2.6).** Hepatocytes were incubated with the derivatives at 25  $\mu\text{M}$  for 24 h. The images were obtained using inverted microscope. A: control (untreated cells); B-E: treatments by MI-D, MI-J, MI-4F and MI-2,4diF, respectively. The scale is indicated by black bars representing 50  $\mu\text{m}$ . The photographs represent three different experiments in triplicate.

doi:10.1371/journal.pone.0130046.g008

**Table 1. Effects of 1,3,4-thiadiazolium derivatives on MDR cell parameters.**

	Pgp				ABCG2				MRP1			
	EC <sub>50</sub>	%inhibition	<sup>a</sup> IG <sub>50</sub>	<sup>b</sup> IG <sub>50</sub>	EC <sub>50</sub>	%inhibition	<sup>a</sup> IG <sub>50</sub>	<sup>b</sup> IG <sub>50</sub>	EC <sub>50</sub>	%inhibition	<sup>a</sup> IG <sub>50</sub>	<sup>b</sup> IG <sub>50</sub>
MI-D	n.d.	1.0	24.9 ± 5.7	9.0 ± 0.2	24.3 ± 9.6	36.7 ± 14.4	7.0 ± 0.1	8.9 ± 1.0	n.d.	8.1 ± 4.2	9.4 ± 0.5	7.5 ± 1.0
MI-J	n.d.	13.6 ± 6.3	9.8 ± 2.0	10.6 ± 0.5	8.5 ± 4.8	21.5 ± 12.1	7.9 ± 0.1	6.0 ± 0.1	n.d.	36.2 ± 24.7	4.9 ± 0.2	5.8 ± 0.1
MI-4F	n.d.	0	3.3 ± 0.1	1.4 ± 0.1	n.d.	11.7 ± 3.9	4.7 ± 0.2	5.7 ± 0.3	n.d.	10.1 ± 6.6	6.2 ± 0.1	6.0 ± 0.1
MI-2,4diF	n.d.	0.15	5.2 ± 0.2	1.0 ± 0.1	n.d.	17.7 ± 12.6	3.3 ± 0.3	4.6 ± 0.9	n.d.	21.0 ± 13.1	4.7 ± 0.5	5.5 ± 0.5

The experimental conditions are described in the Materials and Methods, sections 2.5.1 and 2.9. The efficiency of each mesoionic derivative to inhibit the efflux of fluorescent substrates was determined by flow cytometry, relatively to controls (either parental cells, or the same transfected cells fully inhibited with reference inhibitors). The EC<sub>50</sub> values ( $\mu\text{M}$ ) were determined by using increasing derivatives concentrations, up to 50  $\mu\text{M}$ , and calculated as derivatives concentrations producing half-maximal inhibition of drug efflux. The IG<sub>50</sub> values ( $\mu\text{M}$ ) were obtained by MTT assays upon treatment for 72 h with mesoionic derivatives at 0–100  $\mu\text{M}$ ; they were calculated as derivatives concentrations producing half-maximal inhibition of growth.

<sup>a</sup>IG<sub>50</sub> obtained with resistant transfected cells

<sup>b</sup>IG<sub>50</sub> obtained with control, sensitive, cells; *n.d.* not determined

doi:10.1371/journal.pone.0130046.t001

more efficient than NO<sub>2</sub> in MI-D (36.2% versus 8.1% inhibition) while the fluorinated derivatives MI-4F and MI-2,4diF displayed intermediate potency (10–20% inhibition).

## Discussion and Conclusions

The present work reports a small series of new compounds as promising candidates for future assays of HCC treatment. The different mesoionic derivatives were cytotoxic to HepG2 cells, as demonstrated by MTT assays, with MI-J, MI-4F and MI-2,4diF being the most efficient to reduce their viability whereas MI-D required a 2-fold higher concentration. These results were confirmed by an increase in LDH activity of cell culture supernatants induced by all derivatives, with however some quantitative differences. The survival of non-tumoral hepatocytes in the presence of mesoionic derivatives demonstrated that MI-D, MI-J and MI-4F were not cytotoxic for these cells. By difference, a significant apparent cytotoxicity was observed with MI-2,4diF, in MTT assays, but no increase was produced on LDH activity. The absence of cytotoxicity was further confirmed by the lack of labeling with annexin V or PI, and by morphological analysis. Pires *et al.* [30] demonstrated that the alterations produced by 1,3,4-thiadiazolium derivatives on mitochondrial bioenergetics were associated with their hydrophobic properties: MI-2,4diF displayed the most pronounced effects, probably due to its high Hansh constant ( $\pi = 0,28$ ) as compared to MI-4F, MI-D and MI-J. Therefore, the significant reduction of non-tumoral cell viability observed with MI-4diF in the MTT assay, which is based on the activity of mitochondrial dehydrogenases [50], might be related to its effects on mitochondrial bioenergetics. Induction of apoptosis by chemotherapeutics is one of the most significant effects related to inhibition of tumor growth [51]. When HepG2 cells were labeled here with annexin V and PI to monitor such an event, all mesoionic derivatives were indeed able to induce a significant double labeling. Annexin V is known to specifically bind to phosphatidylserine, a lipid which is translocated to the outer leaflet of the cell during apoptosis and can be identified through FITC fluorescence associated to annexin V [52]. PI is impermeable to cell membrane and its binding to DNA is dependent on the increased membrane permeability observed in the late stages of apoptosis or necrosis [53]. The results obtained with mesoionic compounds indicated that they induced a late apoptosis or necrosis in HepG2 cells. In order to better characterize the cytotoxicity pathway promoted, the HepG2 cells were incubated with the mesoionic derivatives, and the morphological analyses in earliest times of incubation indicated apoptosis features. These data were also confirmed by DNA fragmentation assays. Similar morphological alterations on melanoma cells MEL-85 were demonstrated with MI-D treatment (25–50  $\mu$ M for 2 h), which also reduced the viability of the cells to ~ 40% at 25  $\mu$ M for 24 h [29]. In this work, we used primary culture of rat hepatocytes instead human cells due the scarce availability of fresh human liver samples, the logistic and time required by the overall procedure, as well as the high cost related to the procedure. As performed in this work, other studies [54–56] also have used rat primary hepatocytes in culture as an alternative to verify differential cytotoxicity of antitumoral compounds on human cancer. Nevertheless, the absence of cytotoxicity in rat cells observed in this work must be further confirmed on human cells. For new drugs intended to be used in clinical trials, several absorption, distribution, metabolism, excretion and toxicity assays are required, and the FDA has recommended initial *in vitro* tests to establish the effects of these drug candidates on MDR transporters, which could either promote their efflux or be inhibited by them, thus changing the bioavailability of other drugs used concomitantly [57]. We experimentally observed that mesoionic derivatives were not substrates of ABCG2 and MRP1, whereas they might indeed be transported by Pgp (except for MI-J), which could limit their use against resistant tumors overexpressing this efflux pump. This however would not prevent their utilization in nonresistant tumor treatment: for example, the chemotherapeutic agent 5-fluoracil is

recognized as a first-choice treatment for nonresistant HCC in advanced stage [58], although displaying a high RR value of 53 on Pgp-overexpressing resistant HepG2 cells [59]. Some drugs with antitumoral and pump-efflux inhibitory activities, as also observed here for most 1,3,4-thiadiazolium derivatives, have indeed given promising results *in vivo*. As an example, the tyrosine kinase inhibitor BIBF120, which has reached phase III clinical trials of cancers treatments, also demonstrated a capacity to inhibit the ABCG2 transporter; however, the direct correlation between such an inhibition and the success of resistant-tumor treatment was not actually established [60]. The weak extent of inhibition by 1,3,4-thiadiazolium derivatives might still represent an advantage, taking into account the reduced probability of bioavailability alterations in polytherapy, and of diminution in the physiological protective role of these efflux pumps [61]. In conclusion, we showed that the 1,3,4-thiadiazolium derivatives MI-D, MI-J, MI-4F and MI-2,4diF were selectively cytotoxic to HepG2 cells, by promoting cell death with apoptosis characteristics, while not affecting the viability of non-tumoral hepatocytes. Furthermore, the 1,3,4-thiadiazolium derivatives were only slightly, or not at all, transported by resistant cells overexpressing ABCG2 and MRP1, while they even produced inhibition of these transporters. Such mesoionic compounds, especially the hydroxy derivative MI-J, might be considered as promising candidates to HCC treatment, either resistant or not, and should encourage new investigations about their mechanisms of action for future clinical tests.

## Author Contributions

Conceived and designed the experiments: GJG ARAP ADP SMSCC. Performed the experiments: GJG ARAP GV AA CEAS AE CMR. Analyzed the data: GJG ARAP GRN GV MEMR GRM ADP SMSCC. Wrote the paper: GJG ARAP ADP SMSCC. Reviewed and edited the manuscript and approved the final version: GJG ARAP GRN GV MEMR GRM ADP SMSCC AA CEAS AE CMR.

## References

1. Shi J, Keller JM, Zhang J, Evan TK. A review on the diagnosis and treatment of hepatocellular carcinoma with a focus on the role of wnts and the dickkopf family of wnt inhibitors. *Journal of Hepatocellular Carcinoma*. 2014; 1:7. PMID: [24639918](#)
2. Padhya KT, Marrero JA, Singal AG. Recent advances in the treatment of hepatocellular carcinoma. *Curr Opin Gastroenterol*. 2013; 29:285–92. doi: [10.1097/MOG.0b013e32835ff1cf](#) PMID: [23507917](#)
3. Jemal A, Bray F, Center MM, Ferlay J, Ward E, Forman D. Global cancer statistics. *CA Cancer J Clin*. 2011; 61:69–90. doi: [10.3322/caac.20107](#) PMID: [21296855](#)
4. Uhl P, Fricker G, Haberkorn U, Mier W. Current status in the therapy of liver diseases. *Int J Mol Sci*. 2014; 15:7500–12. doi: [10.3390/ijms15057500](#) PMID: [24786290](#)
5. Cheng JW, Lv Y. New progress of non-surgical treatments for hepatocellular carcinoma. *Med Oncol*. 2013; 30:381. doi: [10.1007/s12032-012-0381-y](#) PMID: [23292867](#)
6. Reataza M, Imagawa DK. Advances in managing hepatocellular carcinoma. *Front Med*. 2014.
7. Loong HH, Yeo W. Microtubule-targeting agents in oncology and therapeutic potential in hepatocellular carcinoma. *Onco Targets Ther*. 2014; 7:575–85. doi: [10.2147/OTT.S46019](#) PMID: [24790457](#)
8. Kratz F, Muller IA, Ryppa C, Warnecke A. Prodrug strategies in anticancer chemotherapy. *ChemMedChem*. 2008; 3:20–53. PMID: [17963208](#)
9. Holohan C, Van Schaeybroeck S, Longley DB, Johnston PG. Cancer drug resistance: an evolving paradigm. *Nat Rev Cancer*. 2013; 13:714–26. doi: [10.1038/nrc3599](#) PMID: [24060863](#)
10. Wu X, Liu L, Zhang Z, Zhang B, Sun H, Chan GL, et al. Selective Protection of Normal Cells During Chemotherapy by RY4 Peptides. *Mol Cancer Res*. 2014.
11. Endicott JA, Ling V. The biochemistry of P-glycoprotein-mediated multidrug resistance. *Annu Rev Biochem*. 1989; 58:137–71. PMID: [2570548](#)
12. Cole SP, Bhardwaj G, Gerlach JH, Mackie JE, Grant CE, Almquist KC, et al. Overexpression of a transporter gene in a multidrug-resistant human lung cancer cell line. *Science*. 1992; 258:1650–4. PMID: [1360704](#)



13. Doyle LA, Yang W, Abruzzo LV, Krogmann T, Gao Y, Rishi AK, et al. A multidrug resistance transporter from human MCF-7 breast cancer cells. *Proc Natl Acad Sci U S A*. 1998; 95:15665–70. PMID: [9861027](#)
14. Noguchi K, Katayama K, Sugimoto Y. Human ABC transporter ABCG2/BCRP expression in chemoresistance: basic and clinical perspectives for molecular cancer therapeutics. *Pharmacogenomics Pers Med*. 2014; 7:53–64. doi: [10.2147/PGPM.S38295](#) PMID: [24523596](#)
15. Brito AF, Mendes M, Abrantes AM, Tralhao JG, Botelho MF. Positron Emission Tomography Diagnostic Imaging in Multidrug-Resistant Hepatocellular Carcinoma: Focus on 2-Deoxy-2-(18F)Fluoro-D-Glucose. *Mol Diagn Ther*. 2014.
16. Seo S, Hatano E, Higashi T, Hara T, Tada M, Tamaki N, et al. Fluorine-18 fluorodeoxyglucose positron emission tomography predicts tumor differentiation, P-glycoprotein expression, and outcome after resection in hepatocellular carcinoma. *Clin Cancer Res*. 2007; 13:427–33. PMID: [17255262](#)
17. Vander Borgh S, Komuta M, Libbrecht L, Katoonizadeh A, Aerts R, Dymarkowski S, et al. Expression of multidrug resistance-associated protein 1 in hepatocellular carcinoma is associated with a more aggressive tumour phenotype and may reflect a progenitor cell origin. *Liver Int*. 2008; 28:1370–80. doi: [10.1111/j.1478-3231.2008.01889.x](#) PMID: [19055643](#)
18. Sukowati CH, Rosso N, Pascut D, Anfusio B, Torre G, Francalanci P, et al. Gene and functional up-regulation of the BCRP/ABCG2 transporter in hepatocellular carcinoma. *BMC Gastroenterol*. 2012; 12:160. doi: [10.1186/1471-230X-12-160](#) PMID: [23153066](#)
19. Chandrakantha B, Isloor AM, Shetty P, Fun HK, Hegde G. Synthesis and biological evaluation of novel substituted 1,3,4-thiadiazole and 2,6-di aryl substituted imidazo [2,1-b] [1,3,4] thiadiazole derivatives. *Eur J Med Chem*. 2014; 71:316–23. doi: [10.1016/j.ejmech.2013.10.056](#) PMID: [24321835](#)
20. Carvalho SA, da Silva EF, Santa-Rita RM, de Castro SL, Fraga CA. Synthesis and antitrypanosomal profile of new functionalized 1,3,4-thiadiazole-2-arylhydrazone derivatives, designed as non-mutagenic megalol analogues. *Bioorg Med Chem Lett*. 2004; 14:5967–70. PMID: [15546709](#)
21. Xiaohe Z, Yu Q, Hong Y, Xiuqing S, Rugang Z. Synthesis, biological evaluation and molecular modeling studies of N-aryl-2-arylthioacetamides as non-nucleoside HIV-1 reverse transcriptase inhibitors. *Chem Biol Drug Des*. 2010; 76:330–9. doi: [10.1111/j.1747-0285.2010.01017.x](#) PMID: [20731670](#)
22. Archana, Srivastava VK, Kumar A. Synthesis of some newer derivatives of substituted quinazolinonyl-2-oxo/thiobarbituric acid as potent anticonvulsant agents. *Bioorg Med Chem*. 2004; 12:1257–64. PMID: [14980637](#)
23. Jubie S, Ramesh PN, Dhanabal P, Kalirajan R, Muruganantham N, Antony AS. Synthesis, antidepressant and antimicrobial activities of some novel stearic acid analogues. *Eur J Med Chem*. 2012; 54:931–5. doi: [10.1016/j.ejmech.2012.06.025](#) PMID: [22770606](#)
24. Khan I, Ali S, Hameed S, Rama NH, Hussain MT, Wadood A, et al. Synthesis, antioxidant activities and urease inhibition of some new 1,2,4-triazole and 1,3,4-thiadiazole derivatives. *Eur J Med Chem*. 2010; 45:5200–7. doi: [10.1016/j.ejmech.2010.08.034](#) PMID: [20828889](#)
25. Kumar H, Javed SA, Khan SA, Amir M. 1,3,4-Oxadiazole/thiadiazole and 1,2,4-triazole derivatives of biphenyl-4-yloxy acetic acid: synthesis and preliminary evaluation of biological properties. *Eur J Med Chem*. 2008; 43:2688–98. doi: [10.1016/j.ejmech.2008.01.039](#) PMID: [18395299](#)
26. Senff-Ribeiro A, Echevarria A, Silva EF, Sanches Veiga S, Oliveira MB. Effect of a new 1,3,4-thiadiazolium mesoionic compound (MI-D) on B16-F10 murine melanoma. *Melanoma Res*. 2003; 13:465–71. PMID: [14512788](#)
27. Grynberg N, Santos AC, Echevarria A. Synthesis and in vivo antitumor activity of new heterocyclic derivatives of the 1,3,4-thiadiazolium-2-aminide class. *Anticancer Drugs*. 1997; 8:88–91. PMID: [9147617](#)
28. Senff-Ribeiro A, Echevarria A, Silva EF, Veiga SS, Oliveira MB. Antimelanoma activity of 1,3,4-thiadiazolium mesoionics: a structure-activity relationship study. *Anticancer Drugs*. 2004; 15:269–75. PMID: [15014361](#)
29. Senff-Ribeiro A, Echevarria A, Silva EF, Franco CR, Veiga SS, Oliveira MB. Cytotoxic effect of a new 1,3,4-thiadiazolium mesoionic compound (MI-D) on cell lines of human melanoma. *Br J Cancer*. 2004; 91:297–304. PMID: [15199390](#)
30. Pires AR, de Oliveira MB, Echevarria A, Silva EF, Rocha ME, Carnieri EG, et al. Comparative study of the effects of 1,3,4-thiadiazolium mesoionic derivatives on energy-linked functions of rat liver mitochondria. *Chem Biol Interact*. 2010; 186:1–8. doi: [10.1016/j.cbi.2010.04.001](#) PMID: [20385111](#)
31. Pires AR, Noleto GR, Echevarria A, dos Reis CM, Rocha ME, Carnieri EG, et al. Interaction of 1,3,4-thiadiazolium mesoionic derivatives with mitochondrial membrane and scavenging activity: Involvement of their effects on mitochondrial energy-linked functions. *Chem Biol Interact*. 2011; 189:17–25. doi: [10.1016/j.cbi.2010.09.030](#) PMID: [20932958](#)

32. Cadena SM, Carnieri EG, Echevarria A, de Oliveira MB. Effect of MI-D, a new mesoionic compound, on energy-linked functions of rat liver mitochondria. *FEBS Lett.* 1998; 440:46–50. PMID: [9862422](#)
33. Cadena SM, Carnieri EG, Echevarria A, de Oliveira MB. Interference of MI-D, a new mesoionic compound, on artificial and native membranes. *Cell Biochem Funct.* 2002; 20:31–7. PMID: [11835268](#)
34. Souza dos Santos AC, Echevarria A. Electronic effects on <sup>13</sup>C NMR chemical shifts of substituted 1,3,4-thiadiazolium salts. *Magnetic Resonance in Chemistry.* 2001; 39:182–6.
35. Seglen PO. Preparation of isolated rat liver cells. *Methods Cell Biol.* 1976; 13:29–83. PMID: [177845](#)
36. Bracht A., Ishii-Iwamoto E.L. and Kelmer-Bracht A.M. O estudo do metabolismo no fígado em perfusão. In: Bracht A. and Ishii-Iwamoto E.L., Eds., *Métodos de Laboratório em Bioquímica*, Editora Manole, São Paulo, 275–289, 2003.
37. Philips HJ. Dye exclusion test for cell viability In: Patterson PPKMK, editor. *Tissue culture methods and applications.* New York: Academic Press; 1973. p. 406–8.
38. Valdameri G, Genoux-Bastide E, Peres B, Gauthier C, Guitton J, Terreur R, et al. Substituted Chromones as Highly Potent Nontoxic Inhibitors, Specific for the Breast Cancer Resistance Protein. *Journal of Medicinal Chemistry.* 2012; 55:966–70. doi: [10.1021/jm201404w](#) PMID: [22165858](#)
39. Martinez L, Arnaud O, Henin E, Tao H, Chaptal V, Doshi R, et al. Understanding polyspecificity within the substrate-binding cavity of the human multidrug resistance P-glycoprotein. *FEBS J.* 2014; 281:673–82. doi: [10.1111/febs.12613](#) PMID: [24219411](#)
40. Cheung CS, Chung KK, Lui JC, Lau CP, Hon PM, Chan JY, et al. Leachianone A as a potential anti-cancer drug by induction of apoptosis in human hepatoma HepG2 cells. *Cancer Lett.* 2007; 253:224–35. PMID: [17379399](#)
41. Reilly TP, Bellevue FH 3rd, Woster PM, Svensson CK. Comparison of the in vitro cytotoxicity of hydroxylamine metabolites of sulfamethoxazole and dapsone. *Biochem Pharmacol.* 1998; 55:803–10. PMID: [9586952](#)
42. Raza H, John A, Benedict S. Acetylsalicylic acid-induced oxidative stress, cell cycle arrest, apoptosis and mitochondrial dysfunction in human hepatoma HepG2 cells. *Eur J Pharmacol.* 2011; 668:15–24. doi: [10.1016/j.ejphar.2011.06.016](#) PMID: [21722632](#)
43. Darzynkiewicz Z, Bruno S, Del Bino G, Gorczyca W, Hotz MA, Lassota P, et al. Features of apoptotic cells measured by flow cytometry. *Cytometry.* 1992; 13:795–808. PMID: [1333943](#)
44. Balasubramanian V, Shukla R, Murugaiyan G, Bhonde RR, Nalini N. Mouse recombinant leptin protects human hepatoma HepG2 against apoptosis, TNF-alpha response and oxidative stress induced by the hepatotoxin-ethanol. *Biochim Biophys Acta.* 2007; 1770:1136–44. PMID: [17543459](#)
45. Douglas RS, Tarshis AD, Pletcher CH Jr., Nowell PC, Moore JS. A simplified method for the coordinate examination of apoptosis and surface phenotype of murine lymphocytes. *J Immunol Methods.* 1995; 188:219–28. PMID: [8551050](#)
46. Bradford MM. A rapid and sensitive method for the quantitation of microgram quantities of protein utilizing the principle of protein-dye binding. *Anal Biochem.* 1976; 72:248–54. PMID: [942051](#)
47. Orrenius S, Nicotera P, Zhivotovsky B. Cell death mechanisms and their implications in toxicology. *Toxicol Sci.* 2011; 119:3–19. doi: [10.1093/toxsci/kfq268](#) PMID: [20829425](#)
48. Hossain MA, Kim DH, Jang JY, Kang YJ, Yoon JH, Moon JO, et al. Aspirin induces apoptosis in vitro and inhibits tumor growth of human hepatocellular carcinoma cells in a nude mouse xenograft model. *Int J Oncol.* 2012; 40:1298–304. doi: [10.3892/ijo.2011.1304](#) PMID: [22179060](#)
49. Hall MD, Handley MD, Gottesman MM. Is resistance useless? Multidrug resistance and collateral sensitivity. *Trends in Pharmacological Sciences.* 2009; 30:546–56. doi: [10.1016/j.tips.2009.07.003](#) PMID: [19762091](#)
50. Takahashi S, Abe T, Gotoh J, Fukuuchi Y. Substrate-dependence of reduction of MTT: a tetrazolium dye differs in cultured astroglia and neurons. *Neurochem Int.* 2002; 40:441–8. PMID: [11821152](#)
51. Raychaudhuri S. How can we kill cancer cells: Insights from the computational models of apoptosis. *World J Clin Oncol.* 2010; 1:24–8. doi: [10.5306/wjco.v1.i1.24](#) PMID: [21603307](#)
52. Vermes I, Haanen C, Steffens-Nakken H, Reutelingsperger C. A novel assay for apoptosis. Flow cytometric detection of phosphatidylserine expression on early apoptotic cells using fluorescein labelled Annexin V. *J Immunol Methods.* 1995; 184:39–51. PMID: [7622868](#)
53. Rieger AM, Nelson KL, Konowalchuk JD, Barreda DR. Modified annexin V/propidium iodide apoptosis assay for accurate assessment of cell death. *J Vis Exp.* 2011; 24:2597.
54. Castaneda F, Kinne RK. Cytotoxicity of millimolar concentrations of ethanol on HepG2 human tumor cell line compared to normal rat hepatocytes in vitro. *J Cancer Res Clin Oncol.* 2000; 126:503–10. PMID: [11003562](#)

55. Tian Z, Si J, Chang Q, Zhou L, Chen S, Xiao P, et al. Antitumor activity and mechanisms of action of total glycosides from aerial part of *Cimicifuga dahurica* targeted against hepatoma. *BMC Cancer*. 2007; 7:237. doi: [10.1186/1471-2407-7-237](https://doi.org/10.1186/1471-2407-7-237) PMID: [18166137](https://pubmed.ncbi.nlm.nih.gov/18166137/)
56. Liu ZH, Zeng S. Cytotoxicity of ginkgolic acid in HepG2 cells and primary rat hepatocytes. *Toxicol Lett*. 2009; 187:131–6. doi: [10.1016/j.toxlet.2009.02.012](https://doi.org/10.1016/j.toxlet.2009.02.012) PMID: [19429255](https://pubmed.ncbi.nlm.nih.gov/19429255/)
57. FDA. Drug Interaction Studies—Study Design, Data Analysis, Implications for Dosing, and Labeling Recommendations. 2012.
58. Uchibori K, Kasamatsu A, Sunaga M, Yokota S, Sakurada T, Kobayashi E, et al. Establishment and characterization of two 5-fluorouracil-resistant hepatocellular carcinoma cell lines. *Int J Oncol*. 2012; 40:1005–10. doi: [10.3892/ijo.2011.1300](https://doi.org/10.3892/ijo.2011.1300) PMID: [22179686](https://pubmed.ncbi.nlm.nih.gov/22179686/)
59. Zheng LH, Bao YL, Wu Y, Yu CL, Meng X, Li YX. Cantharidin reverses multidrug resistance of human hepatoma HepG2/ADM cells via down-regulation of P-glycoprotein expression. *Cancer Lett*. 2008; 272:102–9. doi: [10.1016/j.canlet.2008.06.029](https://doi.org/10.1016/j.canlet.2008.06.029) PMID: [18703276](https://pubmed.ncbi.nlm.nih.gov/18703276/)
60. Xiang QF, Wang F, Su XD, Liang YJ, Zheng LS, Mi YJ, et al. Effect of BIBF 1120 on reversal of ABCB1-mediated multidrug resistance. *Cell Oncol (Dordr)*. 2011; 34:33–44. doi: [10.1007/s13402-010-0003-7](https://doi.org/10.1007/s13402-010-0003-7) PMID: [21290212](https://pubmed.ncbi.nlm.nih.gov/21290212/)
61. Stacy AE, Jansson PJ, Richardson DR. Molecular pharmacology of ABCG2 and its role in chemoresistance. *Mol Pharmacol*. 2013; 84:655–69. doi: [10.1124/mol.113.088609](https://doi.org/10.1124/mol.113.088609) PMID: [24021215](https://pubmed.ncbi.nlm.nih.gov/24021215/)